Atmos. Chem. Phys. Discuss., 12, 19423–19454, 2012
www.atmos-chem-phys-discuss.net/12/19423/2012/
doi:10.5194/acpd-12-19423-2012
© Author(s) 2012. CC Attribution 3.0 License.

Atmospheric Chemistry and Physics Discussions

This discussion paper is/has been under review for the journal Atmospheric Chemistry and Physics (ACP). Please refer to the corresponding final paper in ACP if available.

The impact of a future H_2-based road transportation sector on the composition and chemistry of the atmosphere – Part 2: Stratospheric ozone

D. Wang[1], W. Jia[1], S. C. Olsen[1], D. J. Wuebbles[1], M. K. Dubey[2], and A. A. Rockett[3]

[1]Department of Atmospheric Sciences, University of Illinois at Urbana-Champaign, Urbana, IL, USA
[2]Earth Systems Observations, Los Alamos National Lab, Los Alamos, NM, USA
[3]Department of Materials Science and Engineering, University of Illinois at Urbana-Champaign, Urbana, IL, USA

Received: 16 March 2012 – Accepted: 19 June 2012 – Published: 6 August 2012

Correspondence to: D. J. Wuebbles (wuebbles@atmos.uiuc.edu)

Published by Copernicus Publications on behalf of the European Geosciences Union.

Abstract

The prospective future adoption of hydrogen to power the road transportation sector could greatly improve tropospheric air quality but also raises the question whether the adoption would have adverse effects on stratospheric ozone. The possibility of these undesirable impacts must be fully evaluated to guide future policy decisions. Here we evaluate the possible impact of a future (2050) H_2-based road transportation sector on stratospheric composition and chemistry, especially on stratospheric ozone, with the MOZART chemical transport model. Since future growth is highly uncertain we evaluate the impact for two world evolution scenarios, one based on a high emitting scenario (IPCC A1FI) and the other on a low emitting scenario (IPCC B1), as well as two technological options: H_2 fuel cells and H_2 internal combustion engines. We assume a H_2 leakage rate of 2.5 % and a complete market penetration of H_2 vehicles in 2050. The model simulations show that a H_2-based road transportation sector would reduce stratospheric ozone concentrations as a result of perturbed catalytic ozone destruction cycles. The magnitude of the impact depends on which growth scenario the world evolves and which H_2 technology option is applied. For the same world evolution scenario, stratospheric ozone decreases more in the H_2 fuel cell scenarios than in the H_2 internal combustion engine scenarios because of the NO_x emissions in the latter case. If the same technological option is applied, the impact is larger in the A1FI emission scenario. The largest impact, a 0.54 % decrease in annual average global mean stratospheric column ozone, is found with a H_2 fuel cell type road transportation sector in the A1FI scenario; whereas the smallest impact, a 0.04 % increase in stratospheric ozone, is found with applications of H_2 internal combustion engine vehicles in the B1 scenario. The impacts of the other two scenarios fall between the above two bounding scenarios. However, the magnitude of these changes is much smaller than the increases in 2050 stratospheric ozone expected as stratospheric ozone recovers due to the limits in ozone depleting substance emissions imposed in the Montreal Protocol.

ACPD

12, 19423–19454, 2012

1 Introduction

Molecular hydrogen (H_2) is being considered as a key energy carrier for transportation systems of the future because it is potentially cleaner and more efficient than fossil fuels. The large-scale adoption of H_2 to replace fossil fuel in the road transportation sector would change the composition of the atmosphere through changes in the emissions of several important chemical species. Atmospheric H_2 concentrations would likely increase due to leakage during its production, transportation and storage processes while emissions of fossil fuel combustion byproducts including nitrogen oxides (NO_x=NO+NO_2), carbon monoxide (CO) and volatile organic compounds (VOCs) would likely decrease.

There have been a number of studies on the possible impacts of such a transition on stratospheric composition and chemistry due to concerns that significant reductions in stratospheric ozone from a H_2 economy would lead to increased UV radiation reaching the surface. However, no consensus has been achieved on how stratospheric ozone would change as a result of application of H_2 technologies. Under a somewhat extreme assumption of more than quadrupled surface H_2 concentration (2.3 ppmv), and with no changes in fossil fuel combustion related emissions, a 2-D coupled chemistry-climate model study by Tromp et al. (2003) found spatial and temporal enhancement of polar ozone holes, leading to ozone depletion of 3 % ~ 8 %, due to lowered stratospheric temperatures, a result of increased stratospheric water vapor from oxidized H_2. Warwick et al. (2004) found a slight increase (0.1 % ~ 0.6 %) in stratospheric ozone, considering associated changes in CO, NO_x, VOCs emissions with H_2 fuel cells in a 2-D chemistry transport model, with an assumed H_2 leakage rate of 5 %. Based on a coupled chemistry-climate model study, Jacobson (2008) reported a 0.41 % increase in global column ozone assuming H_2 fuel cell vehicles with their associated decrease in fossil fuel combustion related emissions and a 3.2 % decrease in atmospheric H_2 concentrations due to a 3 % leakage rate.

ACPD
12, 19423–19454, 2012

In these previous studies the transition to H_2 technology was assumed to take place immediately with the then current (ca. 2000) background atmosphere. In the real world, however, this transition will take some time to occur, because the industry of H_2 production and the infrastructure of H_2 delivery are not ready, and several technological barriers need yet to be tackled. Considering these facts we assume a gradual rather than an abrupt transition to a H_2 powered road transportation sector. We assume that the transition of the road transportation sector to H_2 power will be complete by 2050. That is, all on-road vehicles operating in 2050 will be powered by H_2. This is particularly relevant to evaluating the stratospheric impacts since the composition of the background atmosphere in 2050 will be different than the current atmosphere especially in regard to the decline of CFCs and other ozone depleting substances due to the implementation of the Montreal Protocol.

We investigate potential changes in catalytic cycles that determine stratospheric ozone concentrations in response to the adoption of a H_2-based road transportation sector assuming a perhaps more realistic H_2 leakage rate of 2.5 % (Schultz et al., 2003; Warwick et al., 2004). Given the uncertainties in projections of future growth and emissions, we evaluate emissions scenarios that encompass several possible growth and technology adoption paths. The growth scenarios are based on the high and low emitting Intergovernmental Panel on Climate Change (IPCC) Special Report on Emissions Scenarios (SRES), A1FI and B1, respectively. The technological adoption scenarios include H_2 fuel cell and H_2 internal combustion engine options. The impacts of these emissions are evaluated using the Model for Ozone and related tracers version 3.1 (MOZART 3.1) three-dimensional chemistry transport model. This is the second paper of two papers on the impacts of a H_2-based road transportation sector with emphasis on the stratospheric ozone, the first focused on tropospheric chemistry (Wang et al., 2012).

ACPD
12, 19423–19454, 2012

2 Emission scenarios

Here we carry out model simulations along with the highest and lowest Intergovernmental Panel on Climate Change (IPCC) Special Report on Emissions Scenarios (SRES) (IPCC, 2000), A1FI and B1, respectively. For each of these two IPCC scenarios a baseline and two H_2 scenarios are further assumed: (1) The Baseline (BL) scenario is the reference scenario for 2050 in which fossil fuel powered vehicles are still the dominant mode of transportation. (2) The H_2 Fuel Cell (H_2-FC) scenario, in which the energy demands of the road transportation sector are met by H_2 fuel cell technology. In this scenario H_2 emissions due to leakage as well as reductions in combustion-related emissions of H_2, NO_x, VOCs, CO and SO_2 are included. (3) The H_2 Internal Combustion Engine (H_2-ICE) scenario, in which the energy demands of the road transportation sector are met by H_2 using internal combustion technology. In this scenario, H_2 emissions due to leakage as well as reductions in combustion-related emissions of H_2, VOCs, CO and SO_2 are included; however, there are no reductions in NO_x emissions because NO_x is still a byproduct of internal combustion process regardless of the type of fuel.

The future emissions of H_2, NO_x, CO, and several NMVOCs (non-methane VOCs) in these assumed scenarios are the same as described in Wang et al. (2012) with the exception of aerosol emissions which are not included in MOZART 3.1; we assume a H_2 : CO mass emission factor of 0.03 for fossil fuel combustion and a H_2 leakage rate of 2.5 %. For more details see Wang et al. (2012). A short description of related emissions is presented here.

Annual global emissions of H_2, CO, NMVOCs and NO_x of current (2000) and 2050 (baseline and H_2 scenarios) are listed in Table 1. Global emissions increase in the 2050 A1FI baseline (A1FI BL) scenario for H_2 (42 %), CO (35 %), NMVOCs (28 %) and NO_x (115 %) relative to 2000. In the 2050 B1 baseline (B1 BL) scenario, global emissions decrease from 2000 for H_2 (19 %), CO (10 %) and NMVOCs (6 %); NO_x emissions increase by 5 %.

ACPD
12, 19423–19454, 2012

In the A1FI scenarios with a H_2 road transportation sector, global H_2 emissions increase by 81 % relative to the 2050 A1FI baseline scenario, or increase by 157 % from the 2000 emissions. Meanwhile, global emissions in the 2050 H_2-FC and H_2-ICE scenarios decrease for CO (25 %), NMVOCs (14 %) and NO_x (29 % in H_2-FC; 0 % in H_2-ICE), compared to the 2050 A1FI baseline scenario. If compared with the 2000 emissions, in a 2050 A1FI world with a H_2 road transportation sector emissions increase, for CO (1.6 %), NMVOCs (10 %) and NO_x (53 % in H_2-FC), to a lesser extent than in the A1FI baseline scenario.

In the B1 scenarios with a H_2 road transportation sector, global H_2 emissions increase by 64 % relative to the 2050 B1 baseline scenario, or increase by 33 % from the 2000 emissions. Concurrently, global emissions in the 2050 H_2-FC and H_2-ICE scenarios decrease for CO (10 %), NMVOCs (8 %) and NO_x (24 % in H_2-FC; 0 % in H_2-ICE), compared to the 2050 B1 baseline scenario. If compared with the 2000 emissions, in a 2050 B1 world with a H_2 road transportation sector emissions decrease, for CO (19 %), NMVOCs (13 %) and NO_x (20 % in H_2-FC), to a greater extent than in the B1 baseline scenario.

These emissions are input to the model as monthly varying maps at the model resolution.

3 Model description

In this study, we evaluate the atmospheric impacts with the Model for OZone And Related chemical Tracers (MOZART) version 3.1 global chemistry transport model. MOZART-3 has been used and evaluated in a number of studies (e.g. Gettelman et al., 2004; Kinnison et al., 2007; Kulawik et al., 2006; Liu et al., 2009, 2011; Pan et al., 2007; Park et al., 2004). The model simulates the atmosphere from the surface to 0.001 Pa level (~115 km) by dividing it vertically into 60 layers. Horizontally the globe is partitioned into 96 grids on latitude and 144 grids on longitude, corresponding to a resolution of 1.9° × 2.5° (latitude × longitude). It simulates in a detailed

ACPD
12, 19423–19454, 2012

fashion the physical and chemical processes of the troposphere and stratosphere. It has 108 species, 71 photochemical reactions, 218 gas phase reactions and 18 heterogeneous reactions including heterogeneous chemistry in the stratosphere and polar stratospheric cloud processes. The model is driven with meteorology from a year of simulation of the Whole-Atmosphere Community Climate Model version 3 (WACCM-3) (Sassi et al., 2004), which represents the mid-1990s atmosphere. This meteorology is repeated for each year for multiyear simulations. We have chosen to use this meteorology since in this study we focus on emissions changes' impacts on photochemistry and because predicting meteorological conditions in 2050 with reasonable confidence is highly difficult. In addition, previous studies (e.g. Lin et al., 2008; Wu et al., 2008) have shown that emissions changes will likely be more important than changes in climate on atmospheric composition and chemistry in the future.

The model is integrated with a time step of 15 min. After completion of one year's calculation, the meteorology field is repeated for the next year. This method allows the impact of changes in emissions to be investigated excluding the possible influences of changes in meteorology. The lower boundary concentrations of CH_4 and N_2O are set to 2.4 ppmv and 0.35 ppmv, respectively, according to the IPCC A1B scenario (IPCC, 2000). Lower boundary conditions for halocarbons are prescribed according to the 2050 concentrations in the Ab baseline scenario developed by the World Meteorological Organization (WMO, 2003). The model is run for 12 yr and has reached steady state. Our analysis is based on results from the last year of simulation.

4 Model results and discussion

In this section we describe and discuss the results of the model simulations. Here the stratosphere refers to the model levels above the tropopause and we adopt the World Meteorological Organization (WMO) definition of tropopause, i.e. the lowest level at which the lapse rate decreases to 2 K km^{-1} or less. Our modeling results show that the combined effect of increased H_2 emissions and other emission changes in a H_2-based

ACPD
12, 19423–19454, 2012

road transport sector would tend to decrease ozone concentrations in the stratosphere in all scenarios except for the B1 H_2-ICE scenario. The overall effects on annually, globally averaged stratospheric column ozone are –0.54 %, –0.23 %, –0.20 % and +0.04 % for A1FI H_2-FC, A1FI H_2-ICE, B1 H_2-FC and B1 H_2-ICE scenarios, respectively. First we will analyze the Baseline scenarios with a fossil fuel based road transportation sector and then the scenarios with H_2 technologies will be discussed and compared with the baseline scenario.

4.1 Baseline scenarios

In the 2050 Baseline simulations stratospheric ozone has recovered to a significant extent compared with today's atmosphere, as would be expected from future decline of atmospheric halogen concentrations. On an annual mean global average basis, stratospheric column ozone increases by ~13 DU (1 Dobson Unit (DU) corresponds to 2.69×10^{20} ozone molecules per square meter) in the 2050 A1FI BL scenario and by ~11 DU in the 2050 B1 BL scenario, from the mid-1990s atmosphere. Figure 1 shows stratospheric column ozone and its increase from the current atmosphere as a function of latitude and time of year in the two baseline scenarios. The increase is not uniform in space and time. The increase is least in the tropics, where stratospheric ozone increases by ~5 DU. Outside the tropics, the increase is generally greater than in the tropics, but bears inter-hemispheric asymmetry; the increase in the Southern Hemisphere is generally greater than in the Northern Hemisphere. The increase in the hemispheric spring is largest throughout a year. Arctic stratospheric column ozone increases by ~20 and ~15 DU in the 2050 A1FI and B1 baseline scenarios. In October and November Antarctic stratospheric column ozone increases by more than 70 DU from the current value (~150 DU) to ~220 DU, signaling a partial but still significant Antarctic ozone hole recovery. These results are within the range reported in WMO (2011). The recovery of the Antarctica ozone hole in October compares well with the average of model simulations in WMO (2011).

ACPD
12, 19423–19454, 2012

4.2 H_2 fuel cell scenarios

The annual mean global average stratospheric column ozone in the A1FI H_2-FC scenario decreases by 0.54 % (~1.5 DU) from the A1FI baseline. In the tropics, zonal mean stratospheric column ozone decreases by less than 1 DU from December to May; whereas it decreases by 1 ~ 1.5 DU from June to November (Fig. 2a). Outside the tropics the reductions are even larger (greater than 1.5 DU). There is a large decrease (more than 2 DU) occurring north of 35° N from September to February, with the maximum reduction of 2.5 DU (0.8 %) appearing at ~40° N in October. There is also a more than 2 DU reduction in the southern mid-latitudes from mid-June to March.

In the B1 H_2-FC scenario the annual, global mean stratospheric column ozone decreases by 0.20 % (~0.5 DU) from the B1 baseline scenario. The pattern of decrease is similar to that in the A1FI scenario, but the magnitude is smaller (Fig. 2b). The decrease in the tropics does not exceed 0.6 DU (or 0.2 %) throughout a year, while the decrease is even smaller (<0.4 DU or 0.15 %) from December to June. Again, there are larger reductions outside the tropics (greater than 0.6 DU or 0.2 %). In the Northern Hemisphere, there is a significant decrease (more than 0.8 DU) present north of 35° N from September to February. In the Southern Hemisphere, there is a band of significant decrease (more than 0.6 DU or 0.2 %) between 30° S and 60° S.

In both the A1FI and B1 H_2-FC scenarios, ozone concentrations are reduced throughout most of the stratosphere; however, there is a layer of slight increase of less than 1 %, or 1×10^{10} molecules cm^{-3} in the middle stratosphere (Fig. 3). This layer of increased ozone is about 10 km thick and starts from ~20 km altitude in the poles and from ~29 km altitude in the tropics. Above this layer in the upper stratosphere, ozone concentrations are reduced by less than 1×10^{10} molecules cm^{-3}, or 1 %. Below the increased ozone layer the ozone concentration reductions are greater as the altitude decreases.

The most significant reductions in annual, zonal mean ozone concentrations are in the upper troposphere/lower stratosphere (UT/LS) region. At each altitude level,

ACPD
12, 19423–19454, 2012

ozone concentrations decreased more near the poles (up to 10×10^{10} molecules cm^{-3} in A1FI and up to 5×10^{10} molecules cm^{-3} in B1) than in the tropics (around 4×10^{10} molecules cm^{-3} in A1FI and around 2×10^{10} molecules cm^{-3} in B1). The relative reduction, however, is greater in the tropics as there is less ozone in the baseline scenario. The maximum zonal mean O_3 relative reduction (up to 10 % in A1FI and up to 5 % in B1) is at approximately 13 km altitude around 15° N. In the lowermost stratosphere, ozone reductions occur partly because of the influence of the underlying troposphere, where ozone concentrations are reduced due to the reduced tropospheric ozone precursor emissions associated with the adoption of H_2 fuel cells (Wang et al., 2012), and partly because local ozone production is reduced as a result of a strong reduction in NO_x concentrations. As shown in Fig. 4, NO_x mixing ratios in the tropical UT/LS region decrease by up to 12 % (75 pptv) in the A1FI and by up to 8 % (30 pptv) in the B1 H_2-FC scenarios relative to their corresponding baseline scenarios. The reduction in the tropical ozone production reduces the amount of ozone transported to the mid-latitudes and the poles. The impact of the tropospheric air and the tropospheric ozone formation mechanism on UT/LS ozone concentrations diminishes with increasing altitude. At higher altitudes, perturbations to the catalytic ozone destruction cycles contribute more to the changes in ozone concentrations.

In the mid-latitude lower stratosphere, it is well established that catalytic cycles involving HO_x dominate local ozone destruction (e.g. Wennberg et al., 1994; WMO, 1995). In these model simulations HO_x catalytic cycles contribute the most to the ozone loss rate in the stratosphere below 20 km altitude at 35° N at the September equinox. HO_x concentrations are predicted to increase by around 3 % ($\sim 1 \times 10^5$ molecules cm^{-3}) and 1 % ($\sim 0.5 \times 10^5$ molecules cm^{-3}) for the A1FI and B1 scenarios, respectively (Fig. 5). As a direct result, the ozone loss cycles catalyzed by HO_x are enhanced.

At the same time, NO_x concentrations are reduced throughout the stratosphere in the H_2-FC scenarios (Fig. 4). The increased stratospheric HO_x concentrations contribute to the reductions in stratospheric NO_x through the reaction

$$OH + NO_2 + M \rightarrow HNO_3 + M \quad \text{(R1)}$$

ACPD
12, 19423–19454, 2012

Additionally, stratospheric NO_x is also likely to be affected by the drastic changes in tropospheric NO_x concentration in the H_2-FC scenarios. The major source of NO_x in the stratosphere is the reaction of N_2O with $O(^1D)$. However, N_2O and $O(^1D)$ concentrations are not significantly affected by the perturbation of a H_2-FC sector. It has been proposed that reactive nitrogen (NO_y) in the upper troposphere over tropical regions can significantly impact lower stratosphere NO_y concentrations (Ko et al., 1986) due to NO_y's longer lifetime than NO_x and strong upwelling in this region. This hypothesis is supported by observations (e.g. Murphy et al., 1993). In this study, NO_y concentrations in the UT/LS region in 2050 are calculated to be about 1 ppbv in all scenarios, exceeding the threshold mixing ratio of 0.6 ppbv suggested by Murphy et al. (1993). Therefore, increased NO_y concentrations in the UT/LS region are likely to impact the stratospheric NO_y abundance. In the H_2-FC scenarios, model results show that NO_y concentrations in the UT/LS region are significantly reduced (by ~15 % for A1FI and by ~8 % for B1), likely leading to decreased NO_x and NO_y in the stratosphere.

Furthermore, the NO_x reduction impacts the HO_x cycles through Reactions (1) and

$$HO_2 + NO \rightarrow OH + NO_2 \quad \text{(R2)}$$

hence affecting HO_x as well as the partitioning between HO_2 and OH. In this case, HO_2 concentrations increase due to decreased availability of NO in Reaction (2), leading to enhanced ozone loss since the rate of HO_x cycles is dependent on HO_2 concentrations to the first order. Meanwhile, the rate of Reaction (1) would fall as NO concentrations decrease, making Reaction (1) a smaller HO_x sink.

Both of these effects tend to further enhance the HO_x cycles. As shown in Fig. 6, the daily average ozone destruction rate by the HO_x cycles at 35° N at the September equinox is increased by 2 % (A1FI) and 1 % (B1) at 20 km altitude (Fig. 6); the total ozone destruction rate by all catalytic cycles increased by 0.5 % (A1FI) and 0.2 % (B1) due to enhanced HO_x cycles.

In addition to promoting the HO_x cycles, a decrease in NO_x concentrations also leads to an enhancement of the halogen cycles via NO_x/halogen cycles coupling. Nevertheless, this enhancement would have a smaller impact on ozone concentrations since

ACPD
12, 19423–19454, 2012

in 2050 halogen cycles are only responsible for a few percent of ozone destruction rate in the lower stratosphere, in which stratospheric halogen loading is expected to be significantly smaller than today's. As shown in Fig. 6, the overall ozone destruction rate is enhanced by 0.1 % in the A1FI and 0.04 % in the B1 scenarios due to the halogen cycles at 35° N at the September equinox at 20 km level. In sum, the decrease in ozone concentrations in the lower stratosphere in the A1FI and B1 H_2-FC scenarios is primarily due to an intensification of the HO_x catalyzed O_3 destruction cycles.

In the middle stratosphere (25–35 km altitude in the tropics, somewhat lower at higher latitudes) annually, zonally averaged ozone concentrations increase by up to 0.4 % in both the A1FI and B1 H_2-FC scenarios (Fig. 3). Even though ozone loss rate due to HO_x catalytic cycles increases due to the previously discussed mechanisms in this region, the overall ozone loss rate is slowed down because NO_x cycles dominate ozone loss in the middle stratosphere and NO_x concentrations are reduced in this region. As shown in Fig. 4, annually, zonally averaged NO_x concentrations decrease by ~3 % (~50 pptv) in the A1FI and by ~2 % (~20 pptv) in the B1 scenario. The NO_x concentration decrease is due to enhancement of Reaction (1), through which increased HO_x concentrations make this Reaction a larger NO_x sink and, likely due to decreases in NO_x concentrations in the underlying atmosphere. The ozone loss rate due to NO_x catalyzed cycles is reduced throughout most of the stratosphere (Fig. 6); however, its impact on ozone concentrations is only significant in the middle stratosphere where NO_x cycles dominate ozone destruction. As shown in Fig. 6, the overall ozone destruction rate at 25 km altitude at 35° N at the September equinox is decreased by 0.35 % in the A1FI and by 0.13 % in the B1 scenario due to the attenuation of the NO_x catalyzed ozone destruction cycles. Therefore, a slight ozone concentration increase is calculated in the middle stratosphere in both the H_2-FC scenarios. The increase in ozone concentration in the middle stratosphere, however, cannot fully compensate the decrease in the lower stratosphere since ozone molecules per unit volume is lower at higher altitude.

ACPD
12, 19423–19454, 2012

In the upper stratosphere, HO_x catalyzed cycles again dominate ozone loss cycles. The HO_x concentrations increase by 2–3 % in the A1FI and by ∼1 % in the B1 scenarios (Fig. 5). This increase is due to enhanced H_2 abundance and the decline in the rate of Reaction (1) as a result of the NO_x concentrations decrease. As a direct result, HO_x catalyzed cycles are enhanced. As shown in Fig. 6, the ozone destruction rate due to HO_x cycles at 25 km altitude at 35° N at the September equinox level is increased by 0.3 % in the A1FI and 0.13 % in the B1 scenarios. The resulting O_3 concentration decline in this region is less than 1 % in the A1FI and B1 H_2-FC scenarios (Fig. 3). Its impact on stratospheric column ozone is small owing to the low molecule concentrations at such high altitudes.

4.3 H_2 internal combustion engine scenarios

The overall impact of a H_2-ICE road transportation sector on stratospheric ozone concentration is smaller compared with the corresponding H_2-FC scenarios mainly because of NO_x being higher for the ICE scenarios. The annually, globally averaged stratospheric column ozone in the A1FI H_2-ICE scenario would be reduced by 0.23 %, or 0.5DU. Stratospheric column ozone decreases north of 50° S but increases south of this latitude (Fig. 7a). In the tropics, stratospheric column ozone decreases by 0.1–0.3 %, or 0–1 DU throughout a year. In the northern mid- and high-latitudes, stratospheric column ozone decreases by more than 1 DU. The greatest decrease (1.5 DU or 0.6 %) occurs at the northern mid-latitudes from September to January. In the Antarctic region, stratospheric column ozone increases by up to 3 DU, or 1 % from October to December.

From the zonal average perspective, annual mean ozone concentrations are reduced in the lower stratosphere in the A1FI H_2-ICE scenario (Fig. 8a). In the tropics, the reduction extends to the middle stratosphere (30 km altitude). The maximum relative reduction (5 %) occurs at 17 km altitude just north of the equator, whereas the largest concentration change (a decrease of 8×10^{10} molecules cm^{-3}) is at 12 km in the Arctic region. There are very slight ozone reductions above 45 km altitude in the tropics and

ACPD
12, 19423–19454, 2012

above 48 km altitude in the poles. Ozone concentrations are increased in the rest of the stratosphere, but the relative increase does not exceed 1 %. There is an increase of up to 8×10^{10} molecules cm^{-3} around 18 km in the Antarctic region.

As in the H_2-FC scenarios, ozone concentration changes in the H_2-ICE scenarios are a result of changes in radical concentrations, which affect the catalytic cycles destructing stratospheric ozone. HO_x concentrations decrease in the upper troposphere due to the reduced NMVOCs emissions in the A1FI H_2-ICE scenario, as NMVOCs oxidation provides a HO_x source in the upper troposphere. Increase in NO_x concentrations (Fig. 10a) also contributes to the HO_x decrease through Reaction (1). This decrease penetrates into the lower stratosphere with rising air from the tropics. Figure 9a shows the pattern of HO_x reductions, which diminish with altitude. Above 20 km in the tropics and above 15 km near the poles, HO_x concentrations increases slightly as the H_2 leaked into the atmosphere provides a HO_x source in the stratosphere.

NO_x concentrations decrease in the middle stratosphere but increase in the upper and lower stratosphere in the A1FI H_2-ICE scenario (Fig. 10a). In the lower stratosphere NO_x concentrations increase because of the NO_x budget increase throughout the troposphere since in the H_2-ICE scenarios NO_x is still emitted as combustion byproduct of internal combustion engines (Wang et al., 2012). Meanwhile, the decrease in HO_x concentrations (Fig. 9a) decreases the NO_x loss due to Reaction (1), which in turn increases NO_x. In the middle stratosphere where HO_x concentrations (Fig. 9a) are increased, the NO_x loss due to Reaction (1) is reduced, resulting in increased NO_x concentrations. The maximum reduction, around 24 pptv, occurs at 35 km level near the equator.

As shown in Fig. 11a, the ozone destruction rate due to HO_x cycles at 35° N at the September equinox increases by 0.4 % to 1.1 % between 20 km and 50 km levels in the A1FI H_2-ICE scenario, a direct result of increased HO_x concentrations. In the middle stratosphere between 28 km and 40 km levels, the increase in the ozone destruction rate due to HO_x cycles is more than 1 %. However, the contribution of HO_x cycles to the total ozone destruction rate is least in the middle atmosphere (Fig. 11b)

ACPD
12, 19423–19454, 2012

because NO_x cycles dominate ozone destruction here. In the upper and lower stratosphere where HO_x cycles dominate, contributions of the HO_x cycles to the total ozone loss rate increase by 0.35 % at 45 km level and by 0.3 % at 21 km level. This intensification is damped and even offset by the attenuation of the NO_x cycles in the lower and middle stratosphere, resulting in reduction in total ozone loss rate between 23 and 30 km levels. The combined impact of the perturbations to different catalytic cycles on ozone is a small in magnitude but spatially widespread ozone concentration increase in the middle stratosphere (Fig. 8a). However, this increase does not fully compensate the decrease in column in the lower stratosphere because ozone is denser in terms of molecular number concentration at lower levels. The global-mean column ozone in the stratosphere would still be 0.23 % less than that in the A1FI BL atmosphere.

In the B1 H_2-ICE scenario the annual, global mean stratospheric column ozone is increased by 0.04 %, or 0.1 DU. Stratospheric column ozone is reduced north of 10° S but is increased south of this latitude throughout the year (Fig. 7b). The decrease in stratospheric column ozone in the Northern Hemisphere is no more than 0.5 DU. There is an increase of up to 3.5 DU, or 1 %, in stratospheric column ozone in the Antarctic region from October to December.

From the zonal mean perspective, annual mean ozone concentrations are reduced in the lower stratosphere in the B1 H_2-ICE scenario (Fig. 8b). The reduction pattern resembles that in the A1FI H2-FC scenario, but the magnitude of reduction is much smaller. The maximum relative reduction (1.5 %) occurs at 17 km altitude, whereas the concentration change is less than 2×10^{10} molecules cm^{-3}. Ozone concentrations are increased in the rest of the stratosphere (except two cells of very slight reduction at 30 km level between 30° S and 60° S and between 30° N and 60° N). There is up to 7×10^{10} molecules cm^{-3}, ~1 %, increase in ozone concentrations at levels around 18 km in the Antarctic region.

Again, HO_x concentrations decrease in the troposphere in the B1 H_2-ICE scenario, for the reason mentioned in discussion of the A1FI H_2-ICE scenario. This decrease in the B1 H_2-ICE scenario is smaller in magnitude compared with that in the A1FI H_2-ICE

ACPD
12, 19423–19454, 2012

scenario, but penetrates higher into the middle stratosphere (Fig. 9b), as the smaller strength of HO_x source from the H_2 leakage emission in the B1 H_2-ICE scenario cannot fully offset the decrease originated in the upper troposphere.

NO_x concentrations increase in the whole stratosphere except a small region in the Southern Hemisphere a few kilometers above the tropopause in the B1 H_2-ICE scenario (Fig. 10b). In the lower stratosphere NO_x concentrations increase as they do in the A1FI H_2-ICE scenario, but again the magnitude of increase is smaller. In the Southern Hemisphere, the changes of NO_x concentrations are in the opposite sign to that of HO_x concentrations (Fig. 9b), indicating a link between HO_x and NO_x concentrations via Reaction (1). In the Northern Hemisphere, NO_x concentrations increase as a result of the widespread decrease in HO_x concentrations (Fig. 9b). The increase in NO_x concentrations in the middle and upper stratosphere can be as much as 20 ppbv, however, the perturbation to the NO_x cycles is relatively small because the baseline NO_x concentrations are high in this region.

In the stratosphere between 20 km and 50 km levels at 35° N at the September equinox, the perturbations to each catalytic cycles are modest (between –0.1 % and +0.3 %) except for the halogen cycles, which decrease by 1.5 % to 2.4 % (Fig. 11c). Despite the NO_x concentration increase (less than 1 %) throughout the stratosphere, the impact of the enhanced NO_x catalyzed cycles on ozone in the lower stratosphere is "buffered" by the decrease in the halogen catalyzed cycles (Fig. 11d). Increased NO_x concentrations lead to slower halogen catalyzed cycles via halogen/NO_x coupling, behaving like a buffer (Nevison et al., 1999). In the upper stratosphere, enhanced HO_x catalyzed cycles are compensated by decreased halogen catalytic cycles. The resulting ozone loss rate is slowed down throughout the stratosphere. Zonal mean ozone concentrations increase slightly throughout the middle and upper stratosphere (Fig. 11b). In the lower stratosphere, ozone decreases in the tropics and the Northern Hemisphere due to tropospheric impact, but increases in the southern high latitudes, where halogen catalyzed ozone loss cycles dominate, and halogen cycles are slowed down in this

ACPD
12, 19423–19454, 2012

region as NO_x concentrations increase. In the B1 H_2-ICE scenario the overall impact on stratospheric column ozone of is minimal (+0.04 %) among the studied H_2 scenarios.

5 Conclusions

In this study the possible impact of a future H_2-based road transportation sector on stratospheric composition and chemistry was investigated through chemistry-climate model simulations of the 2050 atmosphere based on several emission scenarios designed to bracket the possible future changes in emissions. These scenarios are based on the IPCC high (A1FI) and low (B1) emitting paths. In addition, the impacts of two H_2 technology options are assessed: utilizing H_2 in fuel cells and utilizing H_2 in internal combustion engines.

These results suggest that future implementation of a H_2-based road transportation sector would perturb stratospheric chemistry, by means of affecting catalytic ozone destruction cycles involving HO_x, NO_x, and halogens. The magnitude of the impact depends on the future growth path as well as the H_2 technology adopted. In general the impact is larger for the A1FI based scenarios than the corresponding B1 based scenarios, and the H_2-FC scenarios result in more ozone loss than the H_2-ICE scenarios. The impact on global stratospheric column ozone is considerable for the A1FI scenarios (–0.54 % for H_2-FC and –0.23 % for H_2-ICE) and for the B1 H_2-FC scenario (–0.20 %) while there is a slight increase (0.04 %) for the B1 H_2-ICE scenario. The largest relative reduction of ozone concentration occurs in the lower stratosphere where HO_x cycles dominate O_3 loss and impact from the underlying troposphere is prominent. In the middle stratosphere ozone concentrations increase slightly while at higher altitudes they either decrease slightly or increase slightly depending on scenarios. These changes have relatively little impact on column ozone since ozone at this level only makes up a small fraction in terms of column ozone, due to the low ozone number concentration there. It is important to note that the chosen emission scenarios are developed

ACPD
12, 19423–19454, 2012

with a 100 % market penetration assumption. Less impact on stratospheric ozone is possible in the case of an intermediate market penetration.

It is important to note that even though a H_2-based road transportation sector is likely to decrease stratospheric ozone, this reduction is considerably less than the ozone recovery due to the reductions in ozone depleting substances, e.g. CFCs, from the atmosphere in 2050. In terms of total column ozone, our results suggest that there would still be 4 % ∼ 5 % more ozone in the 2050 atmosphere with a H_2-based road transportation sector than that in today's atmosphere. Therefore, the ozone reduction due to a H_2-based road transportation sector should not constitute a major concern on stratospheric ozone and increased UV radiation at the surface in 2050.

Acknowledgements. The authors thank Hugh Pitcher for providing projections of energy efficiency. Funding for this study was provided by the United States Department of Energy through award number DE-FC36-07GO17109 to the University of Illinois project "Evaluation of the Potential Environmental Impacts from Large-Scale Use and Production of Hydrogen in Energy and Transportation Applications". MKD would like to thank LANL's IGPP program for support.

References

Gettelman, A., Kinnison, D. E., Dunkerton, T. J., and Brasseur, G. P.: Impact of monsoon circulations on the upper troposphere and lower stratosphere, J. Geophys. Res., 109, D22101, doi:10.1029/2004JD004878, 2004.

Granier, C., Lamarque, J. F., Mieville, A., Muller, J. F., Olivier, J., Orlando, J., Peters, J, Petron, G., Tyndall, G., and Wallens, S.: POET, a database of surface emissions of ozone precursors, available at: http://www.aero.jussieu.fr/projet/ACCENT/POET.php, 2005.

Intergovernmental Panel on Climate Change (IPCC): Special Report on Emissions Scenarios. Working Group III, IPCC, Cambridge University Press, Cambridge, 2000.

Jacobson, M. Z.: Effects of wind-powered hydrogen fuel cell vehicles on stratospheric ozone and global climate, Geophys. Res. Lett., 35, L19803, doi:10.1029/2008GL035102, 2008.

Kinnison, D. E., Brasseur, G. P., Walters, S., Garcia, R. R., Marsh, D. R., Sassi, F., Harvey, V. L., Randall, C. E., Emmons, L., Lamarque, J. F., Hess, P., Orlando, J. J., Tie, X. X., Randel, W.,

ACPD

12, 19423–19454, 2012

Pan, L. L., Gettelman, A., Granier, C., Diehl, T., Niemeier, U., and Simmons, A. J.: Sensitivity of chemical tracers to meteorological parameters in the MOZART-3 chemical transport model, J. Geophys. Res., 112, D20302, doi:10.1029/2006JD007879, 2007.

Ko, M. K. W., Mcelroy, M. B., Weisenstein, D. K., and Sze, N. D.: Lightning: a possible source of stratospheric odd nitrogen, J. Geophys. Res., 91, 5395–5404, 1986.

Kulawik, S. S., Worden, H., Osterman, G., Luo, M., Beer, R., Kinnison, D. E., Bowman, K. W., Worden, J., Eldering, A., Lampel, M., Steck, T., and Rodgers, C. D.: TES atmospheric profile retrieval characterization: an orbit of simulated observations, IEEE Trans. Geosci. Rem. Sens., 44, 1324–1333, 2006.

Lin, J. T., Patten, K. O., Hayhoe, K., Liang, X. Z., and Wuebbles, D. J.: Effects of future climate and biogenic emissions changes on surface ozone over the United States and China, J. Appl. Met., 47, 1888–1909, 2008.

Liu, C., Liu, Y., Cai, Z., Gao, S., Lu, D., and Kyrola, E.: A Madden-Julian Oscillation-triggered record ozone minimum over the Tibetan Plateau in December 2003 and its association with stratospheric "low-ozone pockets", Geophys. Res. Lett., 36, L15830, doi:10.1029/2009GL039025, 2009.

Liu, Y., Liu C., Tie, X., and Gao S.: Middle stratospheric polar vortex ozone budget during the warming Arctic winter, 2002–2003, Adv. Atmos. Sci., 28, 985–996, 2011.

Murphy, D. M., Fahey, D. W., Proffitt, M. H., Liu, S. C., Chan, K. R., Eubank, C. S., Kawa, S. R., and Kelly, K. K.: Reactive nitrogen and its correlation with ozone in the lower stratosphere and upper troposphere, J. Geophys. Res., 98, 8751–8773, 1993.

Nevison, C. D., Solomon, S., and Gao, R. S.: Buffering interactions in the modeled response of stratospheric O_3 to increased NO_x and HO_x, J. Geophys. Res., 104, 3741–3754, 1999.

Pan, L. L., Wei, J. C., Kinnison, D. E., Garcia, R. R., Wuebbles, D. J., and Brasseur, G. P.: A set of diagnostics for evaluating chemistry-climate models in the extratropical tropopause region RID A-9296-2008, J. Geophys. Res., 112, D09316, doi:10.1029/2006JD007792, 2007.

Park, M., Randel, W., Kinnison, D., Garcia, R., and Choi, W.: Seasonal variation of methane, water vapor, and nitrogen oxides near the tropopause: satellite observations and model simulations, J. Geophys. Res., 109, D03302, doi:10.1029/2003JD003706, 2004.

Sassi, F., Boville, B. A., Kinnison, D., and Garcia, R. R.: The effects of interactive ozone chemistry on simulations of the middle atmosphere, Geophys. Res. Lett., 32, L07811, doi:10.1029/2004GL022131, 2005.

ACPD
12, 19423–19454, 2012

Schultz, M. G., Diehl, T., Brasseur, G. P., and Zittel, W.: Air pollution and climate-forcing impacts of a global hydrogen economy, Science, 302, 624–627, 2003.
Tromp, T. K., Shia, R. L., Allen, M., Eiler, J. M., and Yung, Y. L.: Potential environmental impact of a hydrogen economy on the stratosphere, Science, 300, 1740–1742, 2003.
Wang, D., Jia, W., Olsen, S. C., Wuebbles, D. J., Dubey, M. K., and Rockett, A. A.: The impact of a future H_2-based road transportation sector on the composition and chemistry of the atmosphere – Part 1: Tropospheric composition and air quality, Atmos. Chem. Phys. Discuss., 12, 19371–19421, doi:10.5194/acpd-12-19371-2012, 2012.
Warwick, N. J., Bekki, S., Nisbet, E. G., and Pyle, J. A.: Impact of a hydrogen economy on the stratosphere and troposphere studied in a 2-D model, Geophys. Res. Lett., 31, L05107, doi:10.1029/2003GL019224, 2004.
Wennberg, P. O., Cohen, R. C., Stimpfle, R. M., Koplow, J. P., Anderson, J. G., Salawitch, R. J., Fahey, D. W., Woodbridge, E. L., Keim, E. R., Gao, R. S., Webster, C. R., May, R. D., Toohey, D. W., Avallone, L. M., Proffitt, M. H., Loewenstein, M., Podolske, J. R., Chan, K. R., and Wofsy, S. C.: Removal of stratospheric O_3 by radicals: in-situ measurements of OH, HO_2, NO, NO_2, ClO, and BrO, Science, 266, 398–404, 1994.
World Meteorological Organization (WMO): Scientific Assessment of Ozone Depletion: 1994, WMO Rep. 37, Geneva, 1995.
World Meteorological Organization (WMO): Scientific Assessment of Ozone Depletion: 2002, WMO Rep. 47, Geneva, 2003.
World Meteorological Organization (WMO): Scientific Assessment of Ozone Depletion: 2010, WMO Rep. 52, Geneva, 2011.
Wu, S., Mickley, L. J., Jacob, D. J., Rind, D., and Streets, D. G.: Effects of 2000–2050 changes in climate and emissions on global tropospheric ozone and the policy-relevant background surface ozone in the United States, J. Geophys. Res., 113, D18312, doi:10.1029/2007JD009639, 2008.

ACPD
12, 19423–19454, 2012

Table 1. Annual-mean global emissions of key species for the scenarios developed for this study.

Species Unit	H_2 $Tg\,yr^{-1}$	CO $Tg\,yr^{-1}$	NO_x $TgN\,yr^{-1}$	NMVOCs $Tg\,yr^{-1}$
2000	40.0	1361.2	43.8	469.6
2050 A1FI BL	56.6	1844.7	94.3	600.9
2050 A1FI H_2-FC	102.7	1383.4	67.2	518.5
2050 A1FI H_2-ICE	102.7	1383.4	94.3	518.5
2050 B1 BL	32.4	1223.3	46.0	442.7
2050 B1 H_2-FC	53.2	1107.1	34.8	408.5
2050 B1 H_2-ICE	53.2	1107.1	46.0	408.5

ACPD
12, 19423–19454, 2012

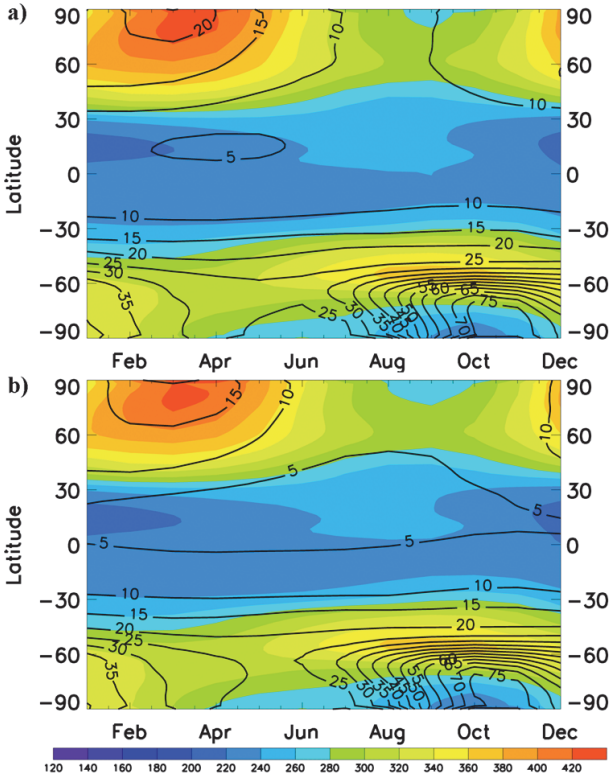

Fig. 1. 2050 zonal mean stratospheric column O_3 (shown by color in units of DU) and the increase from today's atmosphere (a model run representing mid-1990s atmosphere) (shown by contours in units of DU) as a function of latitude and time of a year for **(a)** A1FI BL and **(b)** B1 BL scenarios.

ACPD
12, 19423–19454, 2012

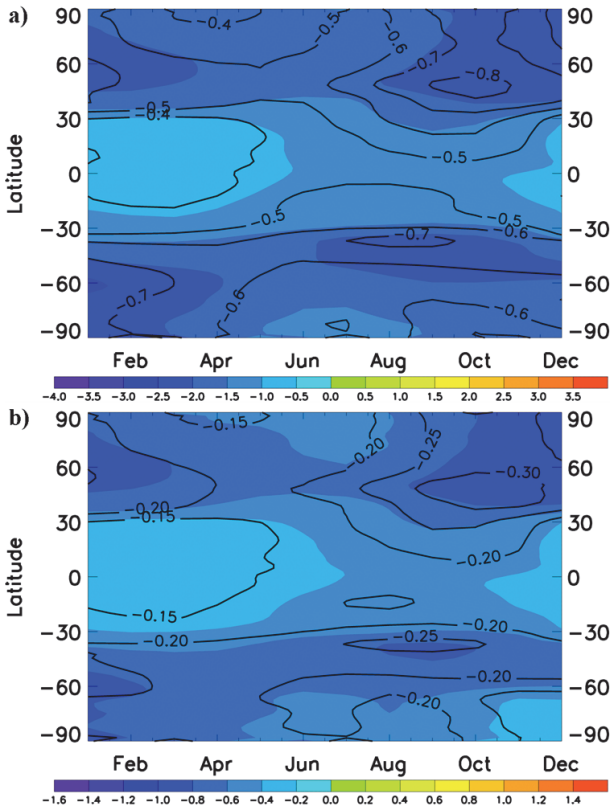

Fig. 2. Zonal mean stratospheric column O_3 changes in units of DU (shown by color) and the relative change in % (shown by contours) in the H_2-FC scenarios compared with the BL scenarios as a function of latitude and time of a year for **(a)** A1FI and **(b)** B1 scenarios.

ACPD
12, 19423–19454, 2012

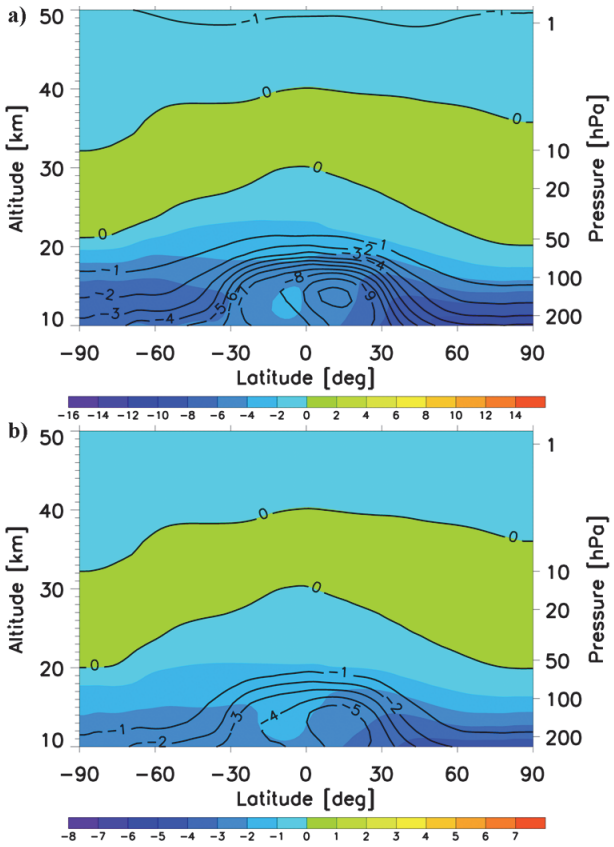

Fig. 3. Annually, zonally averaged O_3 concentration changes in units of 10^{10} molecules cm^{-3} (shown by color) and the relative change in % (shown by contours) in the H_2-FC scenarios compared with the BL scenarios as a function of latitude and altitude for **(a)** A1FI and **(b)** B1 scenarios.

ACPD
12, 19423–19454, 2012

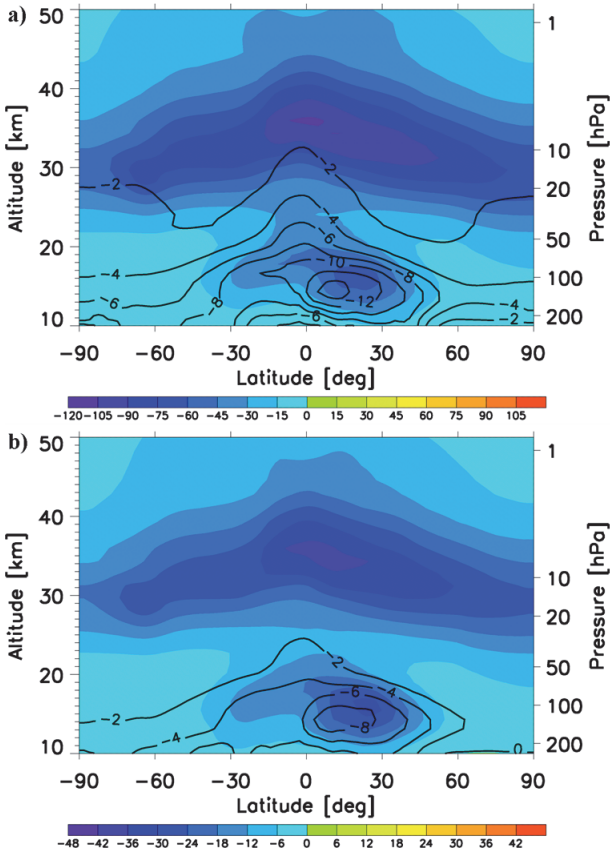

Fig. 4. Annually, zonally averaged NO_x concentration changes in units of pptv (shown by color) and the relative change in % (shown by contours) in the H_2-FC scenarios compared with the BL scenarios as a function of latitude and altitude for **(a)** A1FI and **(b)** B1 scenarios.

ACPD
12, 19423–19454, 2012

Part 2: Stratospheric ozone

D. Wang et al.

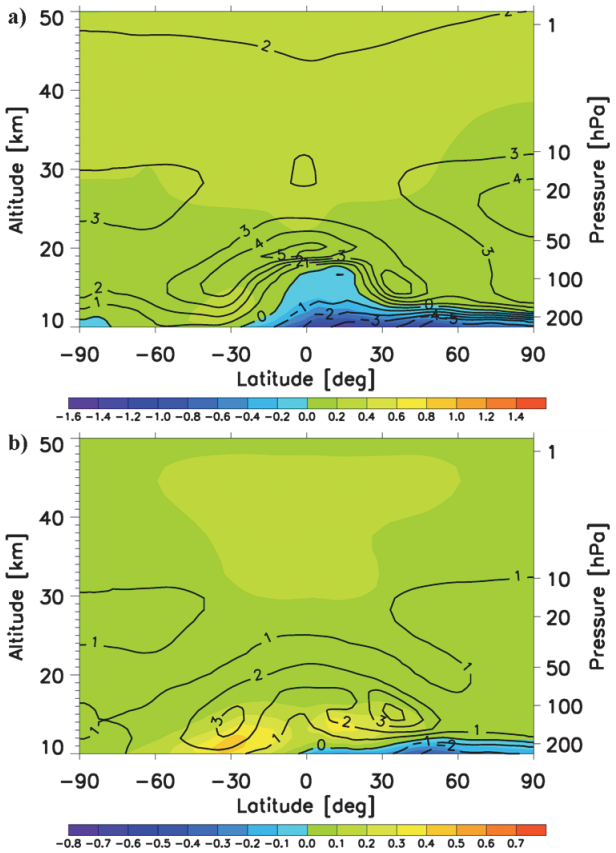

Fig. 5. Annually, zonally averaged HO_x concentration changes in units of 10^6 molecules cm^{-3} (shown by color) and the relative change in % (shown by contours) in the H_2-FC scenarios compared with the BL scenarios as a function of latitude and altitude for **(a)** A1FI and **(b)** B1 scenarios.

ACPD
12, 19423–19454, 2012

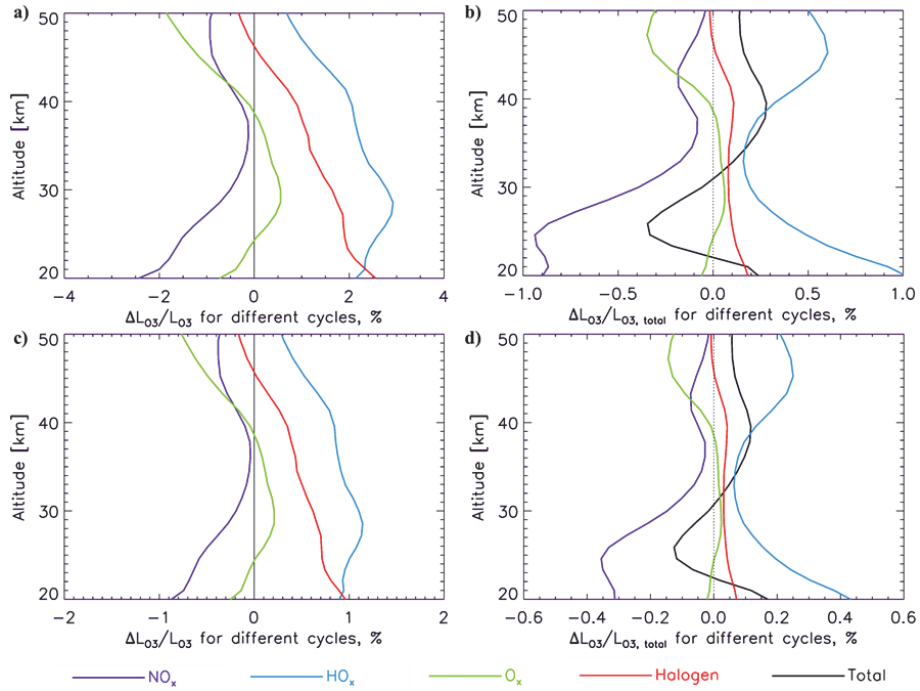

Fig. 6. Changes in contributions of different catalytic O_3 destruction cycles to the total O_3 loss in the H_2-FC scenarios compared to the Baseline scenario. Panels **(a)** and **(b)** are for A1FI and panels **(c)** and **(d)** are for B1. (**a** and **c**) % change in contribution of each catalytic cycle compared to its contribution in the BL; (**b** and **d**) % change in contributions of different catalytic O_3 destruction cycles compared to the total O_3 loss rate in BL. All figures are daily averaged values for the September equinox at 35° N.

ACPD
12, 19423–19454, 2012

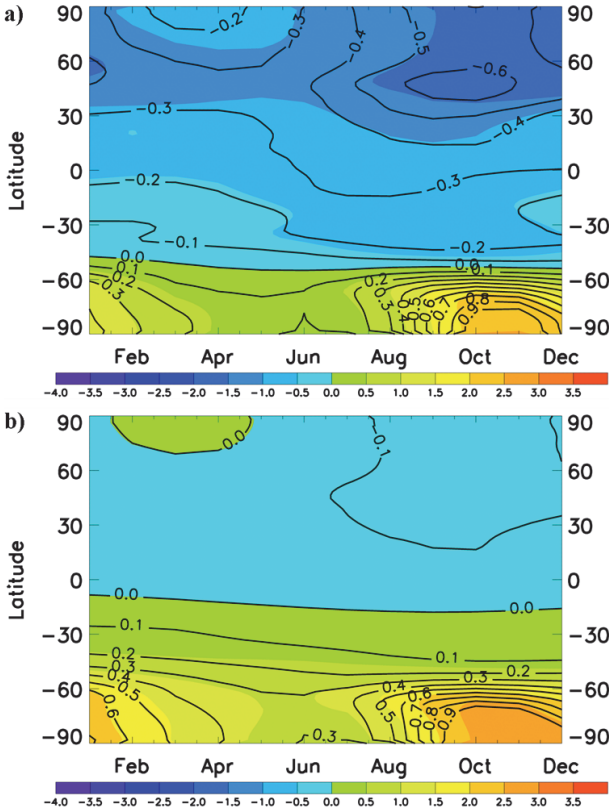

Fig. 7. Zonal mean stratospheric column O_3 changes in units of DU (shown by color) and the relative change in % (shown by contours) in the H_2-ICE scenarios compared with the BL scenarios as a function of latitude and time of a year for **(a)** A1FI and **(b)** B1 scenarios.

ACPD
12, 19423–19454, 2012

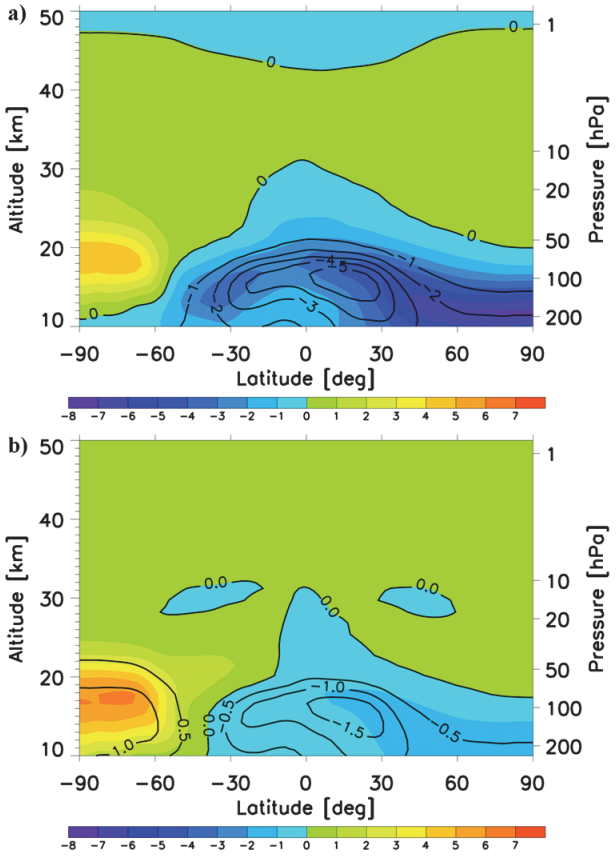

Fig. 8. Annually, zonally averaged O_3 concentration changes in units of 10^{10} molecules cm^{-3} (shown by color) and the relative change in % (shown by contours) in the H_2-ICE scenarios compared with the BL scenarios as a function of latitude and altitude for **(a)** A1FI and **(b)** B1 scenarios.

ACPD
12, 19423–19454, 2012

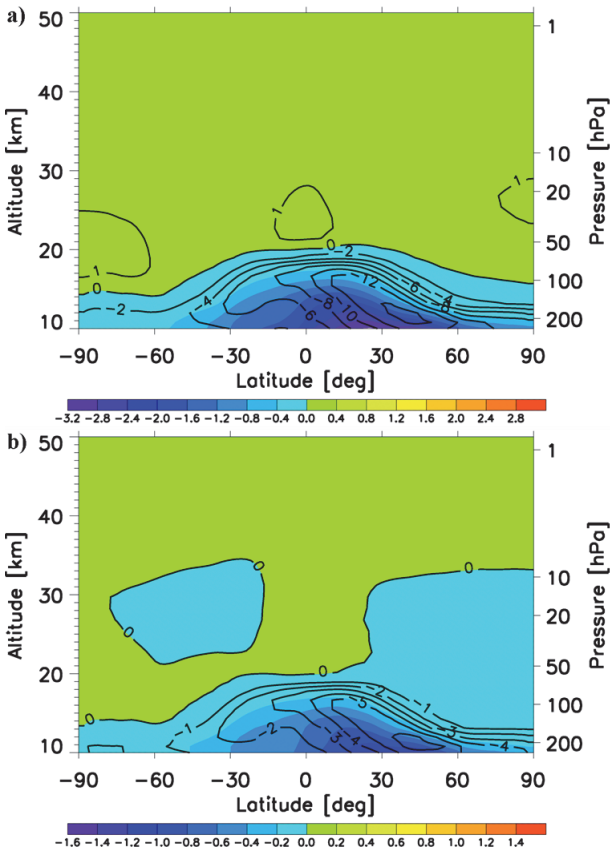

Fig. 9. Annually, zonally averaged HO_x concentration changes in units of 10^6 molecules cm^{-3} (shown by color) and the relative change in % (shown by contours) in the H_2-ICE scenarios compared with the BL scenarios as a function of latitude and altitude for **(a)** A1FI and **(b)** B1 scenarios.

ACPD
12, 19423–19454, 2012

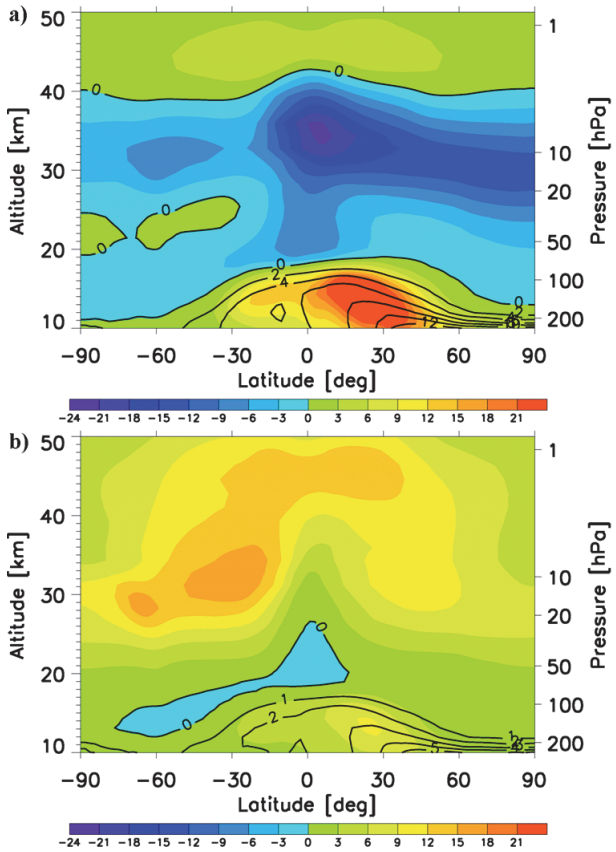

Fig. 10. Annually, zonally averaged NO_x concentration changes in units of pptv (shown by color) and the relative change in % (shown by contours) in the H_2-ICE scenarios compared with the BL scenarios as a function of latitude and altitude for **(a)** A1FI and **(b)** B1 scenarios.

ACPD
12, 19423–19454, 2012

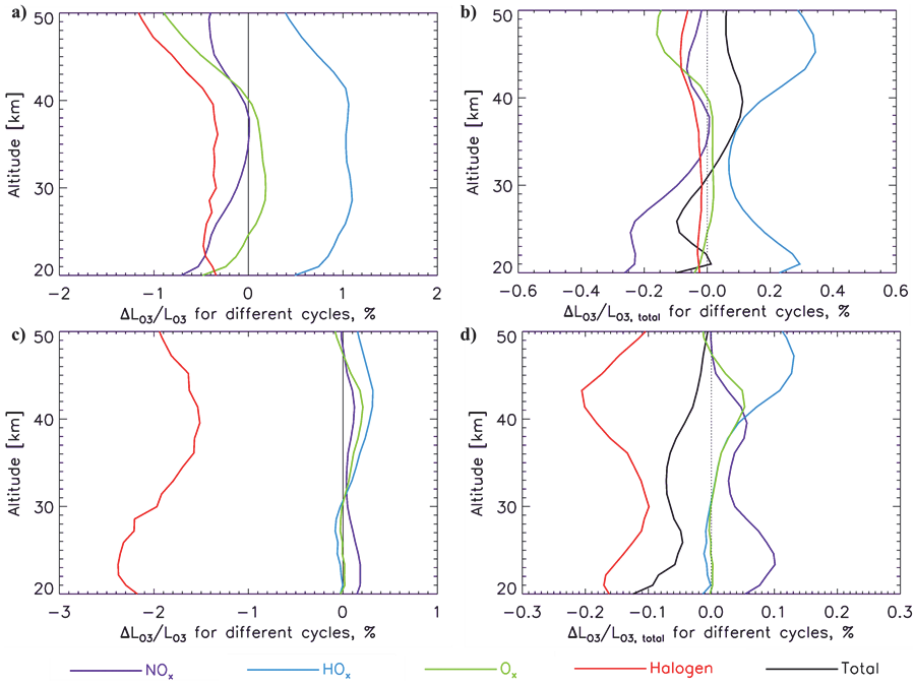

Fig. 11. Changes in contributions of different catalytic O_3 destruction cycles to the total O_3 loss in the H_2-ICE scenarios compared to the Baseline scenario. Panels **(a)** and **(b)** are for A1FI and panels **(c)** and **(d)** are for B1. (**a** and **c**) % change in contribution of each catalytic cycle compared to its contribution in the BL; (**b** and **d**) % change in contributions of different catalytic O_3 destruction cycles compared to the total O_3 loss rate in BL. All figures are daily averaged values for the September equinox at 35° N.

ACPD
12, 19423–19454, 2012